

1   **Title: A derivation error that affects carbon balance models exists in the current implementation of**  
2   **the Johnson et al. (1942) modified Arrhenius function**

3   **Running Title: Derivation error in modified Arrhenius model**

4   Author: Bridget Murphy<sup>1</sup>, Joseph R. Stinziano<sup>2,\*</sup>

5   Affiliations: <sup>1</sup> Department of Biology, University of Western Ontario, London, ON, Canada;

6   <sup>2</sup> Department of Biology, University of New Mexico, Albuquerque, NM, USA

7  
8   \* Corresponding author; Email: jstinziano@unm.edu; Tel: +1 (226) 678-1670

9  
10   Article Type: Modelling/Theory

11   Word Count: 3,146

12   Introduction: 530

13   Description: 1321

14   Results: 671

15   Discussion: 598

16   Acknowledgments: 26

17   Number of Tables: 2

18   Number of Figures: 4

19   Supplementary Files: 1

20

## 21 **Summary**

- 22 • Understanding biological temperature responses is crucial to predicting global carbon fluxes.  
23 The current approach to modelling temperature responses of photosynthetic capacity in large  
24 scale modelling efforts uses a modified Arrhenius equation.
- 25 • We rederived the modified Arrhenius equation from the source publication from 1942 and  
26 uncovered a missing term that was completely dropped by 2002. We compare fitted  
27 temperature response parameters between the new and old derivation of the modified  
28 Arrhenius equation.
- 29 • We find that most parameters are minimally affected, though activation energy is impacted  
30 quite substantially. We then scaled the impact of these small errors to whole plant carbon  
31 balance and found that the impact of the rederivation of the Arrhenius on modelled daily  
32 carbon gain causes a meaningful deviation of  $\sim 18\% \text{ day}^{-1}$ .
- 33 • This suggests that the error in the derivation of the modified Arrhenius equation has impacted  
34 the accuracy of predictions of carbon fluxes at larger scales. We recommend that the  
35 derivation error be corrected in modelling efforts moving forward.

36 *Keywords: Arrhenius, temperature, photosynthesis, gas exchange, modelling, carbon balance*

## Introduction

Globally, photosynthesis and autotrophic respiration are the largest biological carbon fluxes, with photosynthesis removing ~120 Gt C year<sup>-1</sup> from the atmosphere and autotrophic respiration releasing ~60 Gt C year<sup>-1</sup> back to the atmosphere (Amthor, 2000; Ciais *et al.*, 2013). Given the temperature sensitivity of these large carbon fluxes (Lombardozzi *et al.*, 2015), understanding how photosynthesis and respiration respond on acute, acclimatory, and adaptive timescales is crucial for predicting vegetative and carbon cycle responses to future global climates (Rogers *et al.*, 2017; Stinziano *et al.*, 2018). Biological temperature responses including photosynthesis and respiration are typically assumed to be exponential or peaked (Way & Yamori, 2014; Smith & Dukes, 2017; Kumarathunge *et al.*, 2019). Exponential responses are usually modelled based on an Arrhenius-type curve (Arrhenius, 1915):

$$f(T) = A \exp\left(\frac{-E_a}{RT}\right) \quad \text{Equation 1,}$$

or equivalently,

$$f(T) = k_{25} \exp\left[\frac{E_a(T-298.15)}{RT298.15}\right] \quad \text{Equation 2}$$

where  $f(T)$  is the rate of the process at temperature  $T$ ,  $A$  is a pre-exponential factor,  $T$  in K,  $k_{25}$  is the rate of the process at 298.15 K,  $E_a$  is the activation energy in J mol<sup>-1</sup>,  $R$  is the universal gas constant of 8.314 J mol<sup>-1</sup> K<sup>-1</sup>, and 298.15 is the reference temperature in K. As for peaked responses, while a few options are available (Kruse *et al.*, 2008; Hobbs *et al.*, 2013; Heskell *et al.*, 2016), the most commonly implemented version is the modified Arrhenius model of Johnson *et al.* (1942) as presented in Medlyn *et al.* (2002):

$$f(T) = k_{25} \exp\left[\frac{E_a(T-298.15)}{RT298.15}\right] \left[ \frac{1 + \exp\left(\frac{298.15\Delta S - H_d}{298.15R}\right)}{1 + \exp\left(\frac{T\Delta S - H_d}{TR}\right)} \right] \quad \text{Equation 3}$$

where  $H_d$  is the deactivation energy in J mol<sup>-1</sup>, and  $\Delta S$  is the entropy of the process in J mol<sup>-1</sup> K<sup>-1</sup>.

Equation 3 is used for modelling the temperature responses of photosynthetic capacity (i.e. maximum carboxylation capacity of rubisco,  $V_{\text{cmax}}$ , maximum electron transport capacity,  $J_{\text{max}}$ , and triose phosphate utilization capacity (TPU); see Rogers *et al.*, 2017 for a review of models using Equation 3). These parameters are then used in ecophysiological studies to understand thermal acclimation of photosynthesis (see Kattge & Knorr, 2007; Smith & Dukes, 2017; and Kumarathunge *et al.*, 2019 for examples). Furthermore, this equation is also used in terrestrial biosphere models to predict the future carbon cycling (e.g. Rogers *et al.*, 2017).

Due to the ubiquity of Equation 3 in modelling temperature responses and the thermal acclimation of photosynthetic capacity (e.g. Kattge & Knorr, 2007; Rogers *et al.*, 2017; Smith & Dukes, 2017; Kumarathunge *et al.*, 2019), we revisited the original Johnson *et al.* (1942) modified Arrhenius function to rederive Equation 3. In the process of this rederivation, we uncovered a term that was completely dropped sometime between Johnson *et al.* (1942) and Medlyn *et al.* (2002) which causes a systematic error in the application of Equation 3 for modelling photosynthetic capacity in individual species (e.g. Medlyn *et al.*, 2002) to modelling global scale carbon uptake (e.g. Rogers *et al.*, 2017). We then refit a freely available dataset (Kumarathunge *et al.*, 2019), with both versions of the modified Arrhenius model, and fed the temperature response fits through a carbon balance model to estimate the impact of the derivation error on modelled plant carbon balance. We predicted that the derivation error would cause substantial variation in fitted temperature response parameters, and that these differences would propagate through to modelled daily carbon balance.

## **Description**

### **Rederivation of the modified Arrhenius equation**

Johnson *et al.* (1942, equation 24) describe the temperature response of the light intensity of a luciferase reaction as:

$$I = \frac{c''T \exp\left(\frac{-\Delta H^\ddagger}{RT}\right)}{1 + \exp\left(\frac{\Delta S}{R}\right) \exp\left(\frac{-\Delta H}{RT}\right)} \quad \text{Equation 4}$$

where  $I$  is the intensity of the luciferase reaction,  $c''$  is not explicitly defined in Johnson *et al.* (1942), but appears to represent a constant based on the derivation of Equation 4,  $T$  is the temperature in K,  $R$  is the universal gas constant of  $8.314 \text{ J mol}^{-1} \text{ K}^{-1}$ ,  $\Delta H^\ddagger$  is the activation energy in  $\text{J mol}^{-1}$ ,  $\Delta H$  is the deactivation energy in  $\text{J mol}^{-1}$ , and  $\Delta S$  is the entropy in  $\text{J mol}^{-1} \text{ K}^{-1}$ . We can relativize the equation to a reference temperature by dividing Equation 4 at a hypothetical temperature by Equation 4 at a standard temperature (i.e.  $25^\circ\text{C}$ ):

$$\frac{I}{I_{25}} = \frac{\left[ \frac{c'' T \exp\left(\frac{-\Delta H^\ddagger}{RT}\right)}{1 + \exp\left(\frac{\Delta S}{R}\right) \exp\left(\frac{-\Delta H}{RT}\right)} \right]}{\left[ \frac{c'' 298.15 \exp\left(\frac{-\Delta H^\ddagger}{298.15R}\right)}{1 + \exp\left(\frac{\Delta S}{R}\right) \exp\left(\frac{-\Delta H}{298.15R}\right)} \right]} \quad \text{Equation 5}$$

Next, rearrange fractions for clarity:

$$\frac{I}{I_{25}} = \left[ \frac{c'' T \exp\left(\frac{-\Delta H^\ddagger}{RT}\right) c'' T e^{\frac{-\Delta H^\ddagger}{RT}}}{c'' 298.15 \exp\left(\frac{-\Delta H^\ddagger}{298.15R}\right) c'' 298.15 e^{\frac{-\Delta H^\ddagger}{298.15R}}} \right] \left[ \frac{1 + \exp\left(\frac{\Delta S}{R}\right) \exp\left(\frac{-\Delta H}{298.15R}\right) 1 + e^{\frac{\Delta S}{R}} e^{\frac{-\Delta H}{298.15R}}}{1 + \exp\left(\frac{\Delta S}{R}\right) \exp\left(\frac{-\Delta H}{RT}\right) 1 + e^{\frac{\Delta S}{R}} e^{\frac{-\Delta H}{RT}}} \right] \quad \text{Equation 6}$$

Cancel out  $c''$ , use exponent rules to simplify:

$$\frac{I}{I_{25}} = \frac{T}{298.15} \exp\left(\frac{-\Delta H^\ddagger}{RT} - \frac{-\Delta H^\ddagger}{R298.15}\right) \left[ \frac{1 + e^{\frac{\Delta S}{R} + \frac{-\Delta H}{R298.15}} \exp\left(\frac{\Delta S}{R} + \frac{-\Delta H}{R298.15}\right)}{1 + e^{\frac{\Delta S}{R} + \frac{-\Delta H}{RT}} \exp\left(\frac{\Delta S}{R} + \frac{-\Delta H}{RT}\right)} \right] \quad \text{Equation 7}$$

Simplify further by setting a common denominator within exponential terms:

$$I = I_{25} \frac{T}{298.15} \exp\left(\frac{-\Delta H^\ddagger 298.15 \mp \Delta H^\ddagger T}{RT 298.15}\right) \left[ \frac{1 + \exp\left(\frac{298.15 \Delta S - \Delta H}{298.15 R}\right)}{1 + \exp\left(\frac{T \Delta S - \Delta H}{TR}\right)} \right] \quad \text{Equation 8}$$

Simplify exponential terms further:

$$I = I_{25} \frac{T}{298.15} \exp\left(\frac{\Delta H^\ddagger (T - 298.15)}{RT 298.15}\right) \left[ \frac{1 + \exp\left(\frac{298.15 \Delta S - \Delta H}{298.15 R}\right)}{1 + \exp\left(\frac{T \Delta S - \Delta H}{TR}\right)} \right] \quad \text{Equation 9}$$

118

119 Harmonizing the notation scheme to that typically used in plant ecophysiology:

120

$$f(T) = k_{25} \frac{T}{298.15} \exp\left(\frac{E_a(T-298.15)}{RT298.15}\right) \left[ \frac{1 + \exp\left(\frac{298.15\Delta S - H_d}{298.15R}\right)}{1 + \exp\left(\frac{T\Delta S - H_d}{TR}\right)} \right] \quad \text{Equation 10}$$

122

123 Note the difference between Equations 3 and 10: the term  $T / 298.15$  is missing from Equation 3.

124 There are several alternative expressions of Equation 4 (e.g. Farquhar *et al.*, 1980; Harley *et al.*, 1986;  
 125 Harley *et al.*, 1992; Harley & Baldocchi, 1995; Lloyd, 1995), however when relativized to a common  
 126 temperature, the equations presented in Farquhar *et al.* (1980), Harley *et al.* (1992), Harley &  
 127 Baldocchi (1995), and Lloyd (1995) are all identical to Eq. 3 when relativized by temperature, while the  
 128 Harley *et al.* (1986) equation is identical to our derivation when relativized to a common temperature  
 129 (see Appendix A for the relativizations of Farquhar *et al.* (1980), Harley *et al.* (1986), and Harley *et al.*  
 130 (1992); Harley & Baldocchi (1995) uses an identical equation to Eq. 18 from Medlyn *et al.* (2002),  
 131 while Lloyd (1995) uses an identical equation to Eq. 17 from Medlyn *et al.* (2002)). This derivation  
 132 error introduces multiple systematic errors. First, errors are introduced into the fitted parameters  $E_a$ ,  
 133  $H_d$ , and  $\Delta S$ . Second,  $k_{25}$  is scaled using the wrong equation, introducing an error in  $f(T)$ . And third,  
 134 acclimation equations describing  $E_a$ ,  $H_d$ , and  $\Delta S$  will then be in error due to errors in the fitted  
 135 parameters at each temperature. Here we focus on the impact of the dropped term on fitted  
 136 temperature response parameters and modelling whole-plant carbon balance.

137

138 **Data analysis**

139 Using A-C<sub>i</sub> curve data compiled in Kumarathunge *et al.* (2019), available from the Kumarathunge *et al.*  
 140 (2018) repository, we used the {fitacis} function from the R package {plantecophys} (Duursma, 2015),  
 141 setting fitmethod = "bilinear", Tcorrect = FALSE, and fitTPU = TRUE, to obtain  $V_{cmax}$  and  $J_{max}$ . We then  
 142 fit Equations 3 and 10 to the data, allowing  $H_d$  to be fit. To ensure that the curves could be fit (i.e. that  
 143 there were enough data to fit 4 parameters), we only used data where A-C<sub>i</sub> curves were measured at  
 144 5 or more temperatures. This reduced the number of candidate temperature responses from 729 to  
 145 403. We used the R package {minpack.lm} (Elzhov *et al.*, 2016), using Equation 2 to obtain starting  
 146 values for  $E_a$  and  $k_{25}$ , while the other initial parameters were  $\Delta S = 0.650 \text{ kJ mol}^{-1} \text{ K}^{-1}$ , and  $H_d$  varying

147 from 1 to 1000 kJ mol<sup>-1</sup>, followed by the {BIC} function to select the best model based on Bayesian  
148 Information Criteria. We obtained 341 and 337 successful  $V_{\text{cmax}}$  temperature response curve fits for  
149 Equations 3 and 10, respectively, and 241 and 242 successful  $J_{\text{max}}$  temperature response curve fits for  
150 Equations 3 and 10, respectively. This resulted in a total of 547 fitted temperature response curves  
151 which we filtered further, requiring that  $E_a$ ,  $\Delta S$ , and  $H_d$  were all positive values and that the  $V_{\text{cmax}}$  and  
152  $J_{\text{max}}$  data were paired, resulting in 196 complete pairs of  $V_{\text{cmax}}$  and  $J_{\text{max}}$  temperature responses for  
153 analysis. The data covered a temperature range from 1 °C to 50 °C across all curves, with a median  
154 range of 14 °C to 42.6 °C.

155

## 156 **Modelling**

157 We modelled the impact of the Equations 3 and 10 on daily net plant carbon balance. Data for leaf  
158 area, root and shoot masses, as well as leaf dark respiration at 25 °C were taken for white spruce  
159 (*Picea glauca*) from Stinziano & Way (2017), while stomatal conductance model parameters were  
160 calculated with the gas exchange data reported in Stinziano & Way (2017). Briefly, Stinziano and Way  
161 (2017) grew white spruce in growth chambers under a simulated autumn treatment based on  
162 temperatures and photoperiods from Trenton, ON, with weekly harvesting of biomass and gas  
163 exchange measurements across 17 weeks as a control treatment, along with a warming treatment  
164 where temperatures were +5 °C of the control, a constant summer day/night temperature with  
165 declining photoperiod, and a constant summer photoperiod with ambient changes in temperature.  
166 Here we only used data from Stinziano & Way (2017) that were from the control treatment. Mean  
167 data were taken from the control treatment at weeks 0 and 12 to provide contrasting biomass  
168 allocation patterns such that week 0 is a low respiration scenario and week 12 is a high respiration  
169 scenario. These different respiration scenarios were used to reduce bias in any conclusions regarding  
170 the impact of Equations 3 and 10 on carbon balance, as the ratio of photosynthesis to respiration may  
171 alter the sensitivity of net carbon balance to the Arrhenius equation used. Root respiration for white  
172 spruce was taken from Weger & Guy (1991) and we assumed that stem respiration was equal to root  
173 respiration (Table 1).

174

175 For the full model structure and equations, please see the accompanying R package  
176 {arrhenius.comparison} ("arrhenius.comparison\_1.0.1.tar.gz"; Stinziano & Murphy, 2020) (see Table 2

177 for equations). Briefly, we linked the Medlyn *et al.* (2011) stomatal conductance model with the  
178 Farquhar *et al.* (1980) C<sub>3</sub> photosynthesis model, assuming infinite mesophyll conductance to CO<sub>2</sub> as  
179 these assumptions were used in fitting the data from Kumarathunge *et al.* (2018). Photosynthetic  
180 capacity, both maximum rubisco carboxylation capacity,  $V_{\text{cmax}}$ , and maximum electron transport rate,  
181  $J_{\text{max}}$  were scaled to temperature using either Equation 3 or 10, while respiration was scaled according  
182 to (Atkin & Tjoelker, 2003). Photosynthesis and respiration were summed across each modelled day  
183 to calculate daily plant carbon assimilation.

184

185 Modelling was performed on 18 total days of environmental data, with three days of data from three  
186 months (17<sup>th</sup> – 19<sup>th</sup> of May, August, and October, 2019) obtained from external irradiance sensors at  
187 the Biotron Experimental Climate Change Research Centre at the University of Western Ontario and  
188 the remaining environmental data from Environment Canada historical climate data for South London  
189 (43.01°N, 81.27°W, altitude: 251 m; temperature range: -0.1 – 27.9 °C) and the rooftop greenhouse at  
190 the University of New Mexico (35.08°N, 106.62°W, altitude: 1587 m; temperature range: 7.2 – 42.2  
191 °C) to capture different levels of environmental variability (Fig. 1).

192

193 Overall, the modelling approach allows us to assess the relative differences between Equations 3 and  
194 10 under a low- and high- respiration scenario across different ranges of seasonal variability.

195

#### 196 *Statistical analysis*

197 Data were analyzed using the {lm} function in R v.3.6.2 (R Core Team, 2019), regressing the data  
198 obtained from Equation 3 against the data obtained from Equation 10 for each of  $V_{\text{cmax},25}$ ,  $J_{\text{max},25}$ ,  
199  $E_{\text{a},V_{\text{cmax}}}$ ,  $E_{\text{a},J_{\text{max}}}$ ,  $\Delta S_{V_{\text{cmax}}}$ ,  $\Delta S_{J_{\text{max}}}$ ,  $H_{\text{d},V_{\text{cmax}}}$ ,  $H_{\text{d},J_{\text{max}}}$ , BIC values for the fits of Equations 3 and 10, daily  
200 photosynthesis, daily net carbon balance, and daily photosynthesis : daily respiration ratios.

201 Intercepts in the regression, when significant, were interpreted as a bias in the parameter, while  
202 deviations in slope from a 1:1 relationship where interpreted as percentage over- or under-  
203 estimation of the parameter (i.e. [parameter slope – 1] · 100 = % estimation error). All p-values were  
204 corrected for multiple testing using the p.adjust() function in R with Holm's method. All code and data  
205 will be made freely available on GitHub upon publication in the {arrhenius.comparison} R package  
206 (Stinziano & Murphy, 2020).



207

208 **Results**209 *Equations 3 and 10 exhibited similar performance*

210 The performance between Equations 3 and 10 for fitting  $V_{\text{cmax}}$  temperature responses were  
 211 essentially identical when assessed based on BIC, with a slope of  $1.001 \pm 0.001$  ( $F_{1,195} = 5.52 \cdot 10^5$ ,  $R^2 =$   
 212  $0.9996$ ,  $P < 2.2 \cdot 10^{-16}$ ; Fig. **2a**), as was the case for  $J_{\text{max}}$  with a slope of  $1.001 \pm 0.001$  ( $F_{1,195} = 2.43 \cdot 10^6$ ,  
 213  $R^2 = 0.9999$ ,  $P < 2.2 \cdot 10^{-16}$ ; Fig. **2b**). However, while some fitted temperature responses appeared  
 214 identical, there were some cases where the fitted shape differed (Figs. **2c-f**).

215

216 Estimates of  $V_{\text{cmax},25}$  were essentially identical between the Equation 3 fitting (y-axis) and the Equation  
 217 10 fitting (x-axis) with a slope of  $1.002 \pm 0.004$  ( $F_{1,195} = 5.84 \cdot 10^4$ ,  $R^2 = 0.9967$ ,  $P < 2.2 \cdot 10^{-16}$ ; Fig. **3e**),  
 218 as was the case for  $J_{\text{max},25}$  with a slope of  $1.001 \pm 0.001$  ( $F_{1,195} = 6.56 \cdot 10^5$ ,  $R^2 = 0.9997$ ,  $P < 2.2 \cdot 10^{-16}$ ;  
 219 Fig. **3f**).  $E_{a,V\text{cmax}}$  was generally underestimated with a slope of  $0.847 \pm 0.024$  and a positive bias of  $9.73$   
 220  $\pm 2.59 \text{ kJ mol}^{-1}$  when using Equation 3 ( $F_{1,194} = 1202$ ,  $R^2 = 0.8610$ ,  $P < 2.2 \cdot 10^{-16}$ ; Fig. **3a**), while  $E_{a,J\text{max}}$   
 221 was underestimated with a slope of  $0.832 \pm 0.013$  and a positive bias of  $5.98 \pm 1.06 \text{ kJ mol}^{-1}$  ( $F_{1,194} =$   
 222  $3834$ ,  $R^2 = 0.9518$ ,  $P < 2.2 \cdot 10^{-16}$ ; Fig. **3b**).  $\Delta S_{V\text{cmax}}$  was essentially identical between Equation 3 and 10  
 223 with a slope of  $1.000 \pm 0.0233$  ( $F_{1,195} = 1849$ ,  $R^2 = 0.9046$ ,  $P < 2.2 \cdot 10^{-16}$ ; Fig. **3c**), as was the case with  
 224  $\Delta S_{J\text{max}}$  with a slope of  $0.988 \pm 0.033$  ( $F_{1,195} = 904$ ,  $R^2 = 0.8226$ ,  $P < 2.2 \cdot 10^{-16}$ ; Fig. **3d**), and  $H_{d,V\text{cmax}}$  with  
 225 a slope of  $1.002 \pm 0.005$  ( $F_{1,195} = 4.12 \cdot 10^4$ ,  $R^2 = 0.9953$ ,  $P < 2.2 \cdot 10^{-16}$ ; Fig. **3g**). However,  $H_{d,J\text{max}}$  was  
 226 underestimated with a slope of  $0.952 \pm 0.024$  and a positive bias of  $31.48 \pm 8.93 \text{ kJ mol}^{-1}$  ( $F_{1,194} = 1592$ ,  
 227  $R^2 = 0.8914$ ,  $P < 2.2 \cdot 10^{-16}$ ; Fig. **3h**).

228

229 *Impacts on modelled net carbon balance*

230 In general, the differences in thermal response parameters were amplified when integrated at the  
 231 whole-plant level. For modelled daily photosynthesis (A), the slope for the low respiration model was  
 232  $0.819 \pm 0.013$  and the intercept was  $0.018 \pm 0.002 \text{ g plant}^{-1} \text{ day}^{-1}$  (Eq. 3 versus Eq. 10; approximately  
 233 18% of modelled A) ( $F_{1,3523} = 4.168 \cdot 10^3$ ,  $R^2 = 0.5418$ ;  $P < 2.2 \cdot 10^{-16}$ ) (Fig. **4a**). For the high respiration  
 234 model of daily A, the slope was  $0.819 \pm 0.013$  and the intercept was  $0.031 \pm 0.003 \text{ g plant}^{-1} \text{ day}^{-1}$   
 235 (approximately 18% of modelled A) ( $F_{1,3523} = 4.168 \cdot 10^3$ ,  $R^2 = 0.5418$ ;  $P < 2.2 \cdot 10^{-16}$ ) (Fig. **4b**). The low  
 236 respiration model of total daily carbon (C) gain had a slope of  $0.836 \pm 0.012$  and an intercept of  $0.012$

237  $\pm 0.001 \text{ g plant}^{-1} \text{ day}^{-1}$  (approximately 16% of modelled C gain) (Eq. 3 versus Eq. 10;  $F_{1,3523} = 4.539 \cdot$   
 238  $10^3$ ,  $R^2 = 0.5629$ ;  $P < 2.2 \cdot 10^{-16}$ ) (Fig. **4c**). The high respiration of total C gain similarly had a slope of  
 239  $0.859 \pm 0.012$  and an intercept of  $0.011 \pm 0.002 \text{ g plant}^{-1} \text{ day}^{-1}$  (approximately 14% of modelled C gain)  
 240 (Eq. 3 versus Eq. 10;  $F_{1,3523} = 5.364 \cdot 10^3$ ,  $R^2 = 0.6035$ ;  $P < 2.2 \cdot 10^{-16}$ ) (Fig. **4d**). The ratio of the total daily  
 241 photosynthesis: respiration (A/R) was also considered when comparing models. The low respiration  
 242 model of A/R had a slope of  $0.982 \pm 0.007$  and the intercept was  $0.146 \pm 0.031$  (approximately 2% of  
 243 modelled A/R) (Eq. 3 versus Eq. 10;  $F_{1,3523} = 2.096 \cdot 10^4$ ,  $R^2 = 0.8561$ ;  $P < 2.2 \cdot 10^{-16}$ ) (Fig. **4e**). The high  
 244 respiration model had a similar slope of  $0.982 \pm 0.007$  and the intercept was  $0.082 \pm 0.017$   
 245 (approximately 2% of modelled A/R) (Eq. 3 versus Eq. 10;  $F_{1,3523} = 2.097 \cdot 10^4$ ,  $R^2 = 0.8562$ ;  $P < 2.2 \cdot 10^{-$   
 246  $16$ ) (Fig. **4f**).

247

## 248 **Discussion**

249 We sought to determine whether the missing term in Equation 3 had a meaningful impact on fitted  
 250 temperature response parameters due to its prevalence in photosynthetic temperature response data  
 251 and vegetation modelling (Kattge & Knorr, 2007; Duursma & Medlyn, 2012; Rogers *et al.*, 2017; Smith  
 252 & Dukes, 2017; Stinziano *et al.*, 2018; Stinziano *et al.*, 2019; Kumarathunge *et al.*, 2019). Our present  
 253 analysis suggests that there is a large impact on  $E_a$  for both  $V_{cmax}$  and  $J_{max}$ , however there were  
 254 minimal impacts on  $k_{25}$ ,  $H_d$ , and  $\Delta S$  (though note that  $H_d$  for  $J_{max}$  was underestimated) (Fig. **3**). In  
 255 general, fitting Equation 3 instead of Equation 10 results in  $E_a$  reductions of around 15% with positive  
 256 bias. These findings are promising in that one of the parameters to which modelled carbon gain is  
 257 particularly sensitive,  $H_d$  (Stinziano *et al.*, 2018), is minimally affected by the missing term. However,  
 258 since temperature responses are non-linear, small changes in the shape of an accelerating curve can  
 259 have a strong impact on the integral of the response (Jensen, 1906; i.e. changes in the shape of the  
 260 temperature response of carbon assimilation can have strong impacts on total carbon fixation).  
 261 Despite fit performance being nearly identical, the differences due to  $E_a$  values between the  
 262 equations led to an 18% reduction in modelled daily photosynthesis for Equation 3 compared to  
 263 Equation 10, leading ~14-16% reduction in modelled net daily carbon gain. Overall, comparisons of  
 264 low-respiration to high-respiration scenarios resulted in similar percent changes in daily C balance  
 265 with similar variation.

266

267 Not only did we compare the impact of the missing term in Equation 3 on different respiration  
268 scenarios, but we also modelled data across a range of environmental conditions to understand the  
269 impact on C balances of plants under different temperature regimes and how these impacts could  
270 scale up in global models. A ~15% reduction in net daily carbon gain is substantial by itself, but this  
271 difference would also be amplified over time for a single plant. Plant growth follows the compound  
272 interest law (Blackman, 1919). As leaf area increases with growth so does the rate of photosynthesis  
273 and thus the amount of carbon available to further increase growth and metabolism, hence why  
274 relative growth rates are commonly utilized in the literature (e.g. Shipley, 1989; Causton, 1991;  
275 Tjoelker *et al.*, 1999; Loveys *et al.*, 2003; Poorter *et al.*, 2012; Pommereng & Anders, 2015). A  
276 reduction of 18% in modelled daily photosynthesis caused by using the modified equation with the  
277 missing term (Eq. 3) would become compounded long-term with plant growth and may result in  
278 underestimations of future carbon uptake. It is thus likely that the differences we observed would  
279 accumulate to even larger carbon flux errors across large spatial and temporal scales with fluctuating  
280 temperatures.

281

282 Based on the above analysis, the impact of the missing term in the modified Arrhenius equation  
283 substantially alters  $E_a$  and net daily carbon balance at a whole-plant level. Given that carbon balance  
284 is the time integral of net CO<sub>2</sub> assimilation, this may lead to substantial impacts over a long time  
285 period. Despite the robust use of Equation 3 (e.g. Kattge & Knorr, 2007; Oikawa *et al.*, 2016; Rogers *et al.*,  
286 2017; Smith & Dukes, 2017; Mercado *et al.*, 2018; Kumarathunge *et al.*, 2019), Equation 3 is still  
287 incorrect. We therefore recommend the switch from Equation 3 to Equation 10 because: 1) Equation  
288 3 is the result of a derivation error, and 2) Equations 3 and 10 lead to different net daily carbon  
289 estimates due to the derivation error, which may currently be compensated by other factors in large-  
290 scale models.

## 291 **Acknowledgments**

292 We would like to thank Wesley J. Noe at the University of New Mexico for providing climate data. This  
293 research was supported by personal funds.

294

## 295 **Author Contributions**

296 Both authors contributed to all aspects of the study.

297

298 **Tables**

299 **Table 1. Parameters used in modelling daily carbon gain.**

Parameter	Group	Value	Reference
Respiration	R <sub>dark</sub>	2.78 µmol m <sup>-2</sup> s <sup>-1</sup>	Stinziano & Way, 2017
	R <sub>day</sub>	0.7 * R <sub>dark</sub>	Ayub <i>et al.</i> , 2011
	R <sub>root</sub>	0.0095 µmol g <sup>-1</sup> s <sup>-1</sup>	Weger & Guy, 1991
	R <sub>stem</sub>	0.0095 µmol g <sup>-1</sup> s <sup>-1</sup>	Assumed
	Q <sub>10</sub>	2.015	Atkin & Tjoelker, 2003
Γ*	25 °C	42.75 µmol mol <sup>-1</sup>	Bernacchi <i>et al.</i> , 2001
	E <sub>a</sub>	37.83 kJ mol <sup>-1</sup>	Bernacchi <i>et al.</i> , 2001
	25 °C	718.4 µmol mol <sup>-1</sup>	Bernacchi <i>et al.</i> , 2001
K <sub>m</sub>	E <sub>a</sub>	65.51 kJ mol <sup>-1</sup>	Bernacchi <i>et al.</i> , 2001
α		0.8	Norman & Campbell, 1998
φ		0.08	Norman & Campbell, 1998
Leaf Area	Low R	0.015 m <sup>2</sup>	Stinziano & Way, 2017
	High R	0.025 m <sup>2</sup>	Stinziano & Way, 2017
Stem Mass	Low R	0.496 g	Stinziano & Way, 2017
	High R	2.523 g	Stinziano & Way, 2017
Root Mass	Low R	0.498 g	Stinziano & Way, 2017
	High R	5.072 g	Stinziano & Way, 2017

300 **Q<sub>10</sub>: thermal sensitivity coefficient; Γ\*: photorespiratory CO<sub>2</sub> compensation point; K<sub>m</sub>: apparent**  
301 **Michaelis-Menten constant for rubisco carboxylation in 21% O<sub>2</sub>/air (i.e. K<sub>c,air</sub>); α: absorbance of**  
302 **photosynthetically activation radiation; φ: maximum quantum efficiency of photosynthetic electron**  
303 **transport; E<sub>a</sub>: activation energy; R<sub>dark</sub>: leaf respiration in the dark; R<sub>day</sub>: leaf respiration in the light;**  
304 **R<sub>root</sub>: root respiration; R<sub>stem</sub>: stem respiration; Low R: low respiration scenario; High R: high**  
305 **respiration scenario.**

306

307 **Table 2. Equations used in modelling daily carbon uptake.**

Equation	Reference
$f(T) = k_{25} Q_{10}^{\frac{T-298.15}{10}}$	Atkin & Tjoelker, 2003
$f(T) = k_{25} e^{\left[ \frac{E_a(T-298.15)}{RT298.15} \right]}$	Arrhenius, 1915
$f(T) = k_{25} e^{\left[ \frac{E_a(T-298.15)}{RT298.15} \right]} \left[ \frac{1 + e^{\frac{298.15\Delta S - H_d}{298.15R}}}{1 + e^{\frac{T\Delta S - H_d}{TR}}} \right]$	Medlyn <i>et al.</i> , 2002

$$f(T) = k_{25} \frac{T}{298.15} e^{\left[ \frac{E_a(T-298.15)}{RT298.15} \right]} \left[ \frac{1 + e^{\frac{298.15\Delta S - H_d}{298.15R}}}{1 + e^{\frac{T\Delta S - H_d}{TR}}} \right]$$

Johnson *et al.*, 1942; this study

$$W_c = V_{cmax} \frac{C_i - \Gamma^*}{C_i + K_m}$$

Farquhar *et al.*, 1980

$$W_j = J \left( \frac{C_i - \Gamma^*}{C_i + 2\Gamma^*} \right)$$

Farquhar *et al.*, 1980; Way *et al.*, 2011

Where J is calculated as the minimum root of:  $\theta J^2 - (0.5\alpha\phi Q_{in} + J_{max})J + 0.5\alpha\phi Q_{in}J_{max} = 0$

$$A_{gross} = \min(W_c, W_j)$$

$$A_{net} = A_{gross} - R_{day}$$

$$g_s = g_0 + 1.6 \left( 1 + \frac{g_1}{\sqrt{VPD}} \right) \left( \frac{A_{net}}{C_a} \right)$$

Medlyn *et al.*, 2011

$$C_i = C_a - 1.6 \frac{A_{net}}{g_s}$$

$$A_{plant} = A_{net} \times LA - R_{dark} \times LA - R_{stem} \times SM \\ - R_{root} \times RM$$

$$C_{balance} = \sum A_{plant} \times 3600 \times \frac{12.01}{1,000,000}$$

**f(T): rate of a process at a given temperature; T: temperature in K; k<sub>25</sub>: rate of a process at 25 °C;**  
**Q<sub>10</sub>: thermal sensitivity coefficient; E<sub>a</sub>: activation energy in kJ mol<sup>-1</sup>; ΔS: entropy parameter in kJ**  
**mol<sup>-1</sup>; H<sub>d</sub>: deactivation energy in kJ mol<sup>-1</sup>; R: universal gas constant in 0.008314 kJ mol<sup>-1</sup> K<sup>-1</sup>; W<sub>c</sub>: rate**  
**of CO<sub>2</sub>-limited carboxylation in μmol m<sup>-2</sup> s<sup>-1</sup>; W<sub>j</sub>: rate of RuBP regeneration-limited carboxylation in**  
**μmol m<sup>-2</sup> s<sup>-1</sup>; V<sub>cmax</sub>: maximum rate of rubisco carboxylation capacity in μmol m<sup>-2</sup> s<sup>-1</sup>; J<sub>max</sub>: maximum**  
**rate of electron transport in μmol m<sup>-2</sup> s<sup>-1</sup>; C<sub>i</sub>: intercellular CO<sub>2</sub> concentration in μmol mol<sup>-1</sup>; Γ\*:**  
**photorespiratory CO<sub>2</sub> compensation point in μmol mol<sup>-1</sup>; K<sub>m</sub>: Michaelis-Menten constant for rubisco**  
**in μmol mol<sup>-1</sup>; α: absorbance of photosynthetically active radiation; φ: maximum quantum**  
**efficiency of electron transport; Q<sub>in</sub>: incident photosynthetically active radiation; A<sub>gross</sub>: gross CO<sub>2</sub>**  
**assimilation in μmol m<sup>-2</sup> s<sup>-1</sup>; A<sub>net</sub>: net CO<sub>2</sub> assimilation in μmol m<sup>-2</sup> s<sup>-1</sup>; R<sub>day</sub>: leaf day respiration in**  
**μmol m<sup>-2</sup> s<sup>-1</sup>; g<sub>s</sub>: stomatal conductance to water in mol m<sup>-2</sup> s<sup>-1</sup>; g<sub>0</sub>: intercept for the Medlyn *et al.***  
**2011 model; g<sub>1</sub>: slope for the Medlyn *et al.* 2011 model; VPD: vapor pressure deficit in kPa; C<sub>a</sub>: CO<sub>2</sub>**  
**concentration at the leaf surface in μmol mol<sup>-1</sup>; A<sub>plant</sub>: whole plant net CO<sub>2</sub> assimilation; LA: leaf**  
**area in m<sup>2</sup>; R<sub>dark</sub>: leaf dark respiration in μmol m<sup>-2</sup> s<sup>-1</sup>; R<sub>stem</sub>: stem respiration in μmol m<sup>-2</sup> s<sup>-1</sup>; R<sub>root</sub>;**

322 root respiration in  $\mu\text{mol m}^{-2} \text{s}^{-1}$ ; SM: stem mass in g; RM: root mass in g;  $C_{\text{balance}}$ : whole plant daily  
323 carbon balance in  $\text{g plant}^{-1} \text{day}^{-1}$ .

324

#### 325 Figure Captions

326 **Figure 1. Environmental data used to drive the model in Table 1 covering 3 days (17<sup>th</sup>, 18<sup>th</sup>, and 19<sup>th</sup>)**  
327 **of 3 months. (a,c,e) Albuquerque, NM, USA (ABQ); (b,d,e) London, ON, Canada (LDN).**  
328 **Environmental parameters include: a,b) temperature; c,d) vapour pressure deficit; and e,f)**  
329 **irradiance ( $Q_{\text{in}}$ ).**

330

331 **Figure 2. Relative performance and fit for Equations 3 and 10 for temperature responses of  $V_{\text{cmax}}$**   
332 **and  $J_{\text{max}}$  based on a,b) Bayesian Information Criterion (BIC), and c-f) visual inspection of curve fits.**

333

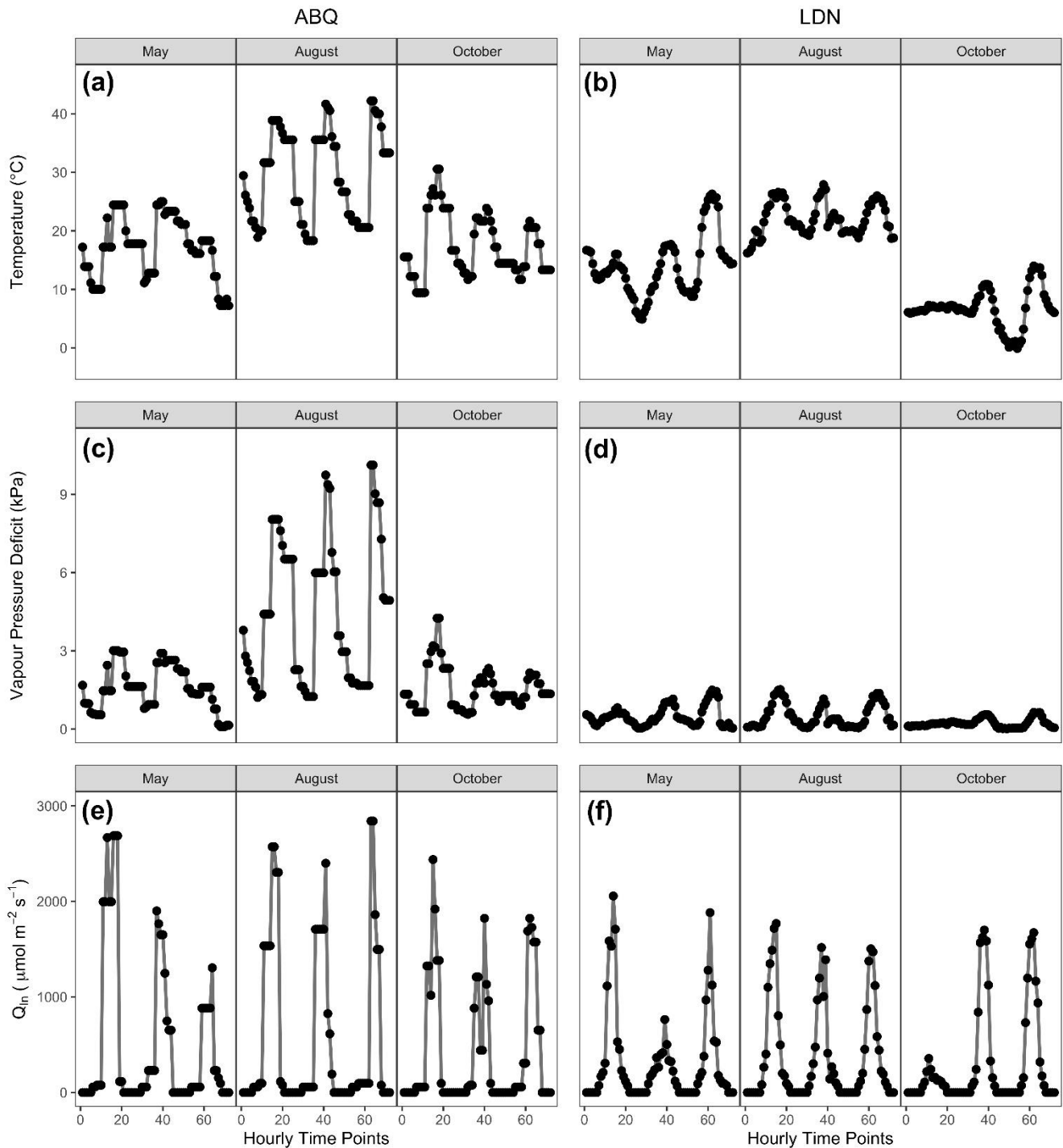
334 **Figure 3. The modified Arrhenius equation missing the term (Equation 3) compared to Equation 10**  
335 **fits different values for  $E_a$  (a,b), but mostly similar values for  $\Delta S$  (c,d),  $k_{25}$  (e,f) and  $H_d$  (f, g) for both**  
336  **$V_{\text{cmax}}$  (a, c, e, g) and  $J_{\text{max}}$  (c, d, f, h).  $E_a$ : activation energy,  $\Delta S$ : entropy parameter,  $k_{25}$ : rate of the**  
337 **process at 25 °C,  $H_d$ : deactivation energy,  $V_{\text{cmax}}$ : maximum capacity of rubisco carboxylation,  $J_{\text{max}}$ :**  
338 **maximum rate of electron transport. Black line indicates 1:1 line and grey dashed line indicates**  
339 **respective modelled slopes and intercepts.**

340

341 **Figure 4. The modified Arrhenius equation without the missing term (Equation 3) gives differences**  
342 **in modelled daily carbon fluxes compared to Equation 10 for low R (a,c,e) and high R (b,d,f) under**  
343 **scenarios where  $H_d$  is allowed to vary. Modelled carbon fluxes include: a,b) Total daily**  
344 **photosynthesis; c,d) total daily C gain; and e,f) total daily A/R. A: photosynthesis, R respiration,**  
345 **Low R: low respiration, High R: high respiration. Black line indicates 1:1 line and grey dashed line**  
346 **indicates respective modelled slopes and intercepts.**

347

#### 348 Figures

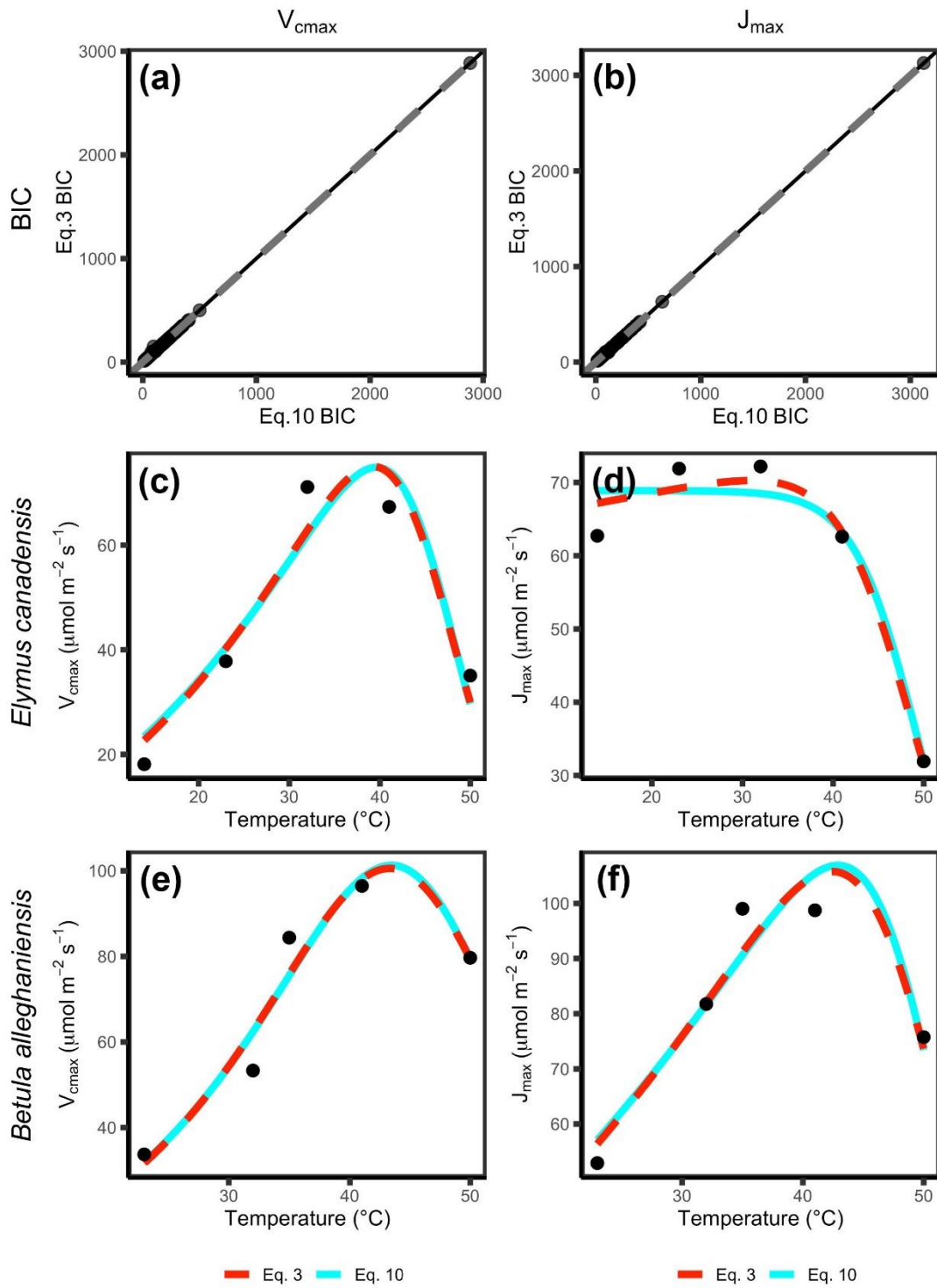


349

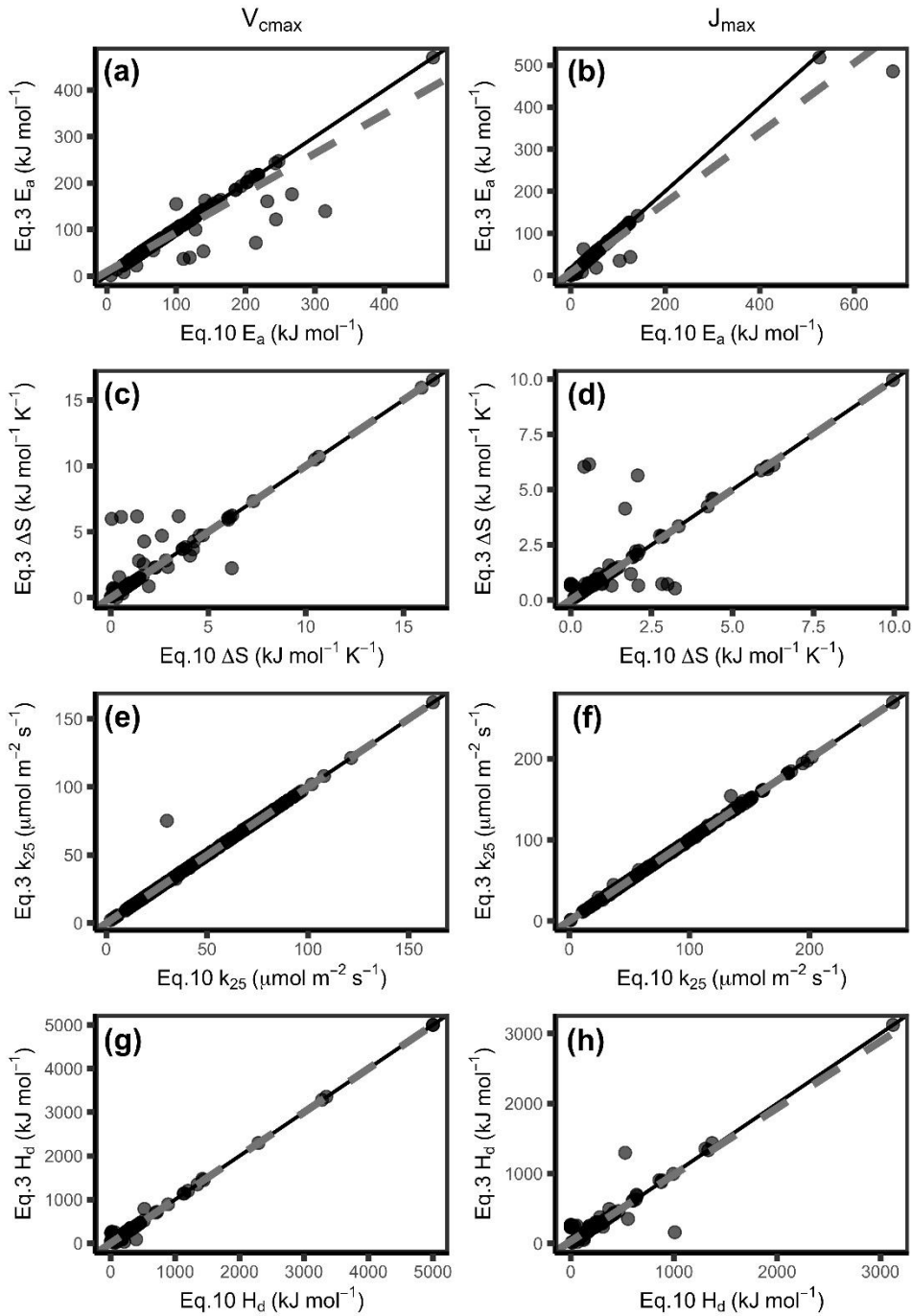
350 **Figure 1. Environmental data used to drive the model in Table 1 covering 3 days (17<sup>th</sup>, 18<sup>th</sup>, and 19<sup>th</sup>)**  
 351 **of 3 months. (a,c,e) Albuquerque, NM, USA (ABQ); (b,d,e) London, ON, Canada (LDN).**

352 **Environmental parameters include: a,b) temperature; c,d) vapour pressure deficit; and e,f)**  
 353 **irradiance ( $Q_{in}$ ).**

354







358

359

360

361

362

363

364

**Figure 3.** The modified Arrhenius equation missing the term (Equation 3) compared to Equation 10 fits different values for  $E_a$  (a,b), but mostly similar values for  $\Delta S$  (c,d),  $k_{25}$  (e,f) and  $H_d$  (f, g) for both  $V_{cmax}$  (a, c, e, g) and  $J_{max}$  (c, d, f, h).  $E_a$ : activation energy,  $\Delta S$ : entropy parameter,  $k_{25}$ : rate of the process at 25 °C,  $H_d$ : deactivation energy,  $V_{cmax}$ : maximum capacity of rubisco carboxylation,  $J_{max}$ : maximum rate of electron transport. Black line indicates 1:1 line and grey dashed line indicates respective modelled slopes and intercepts.

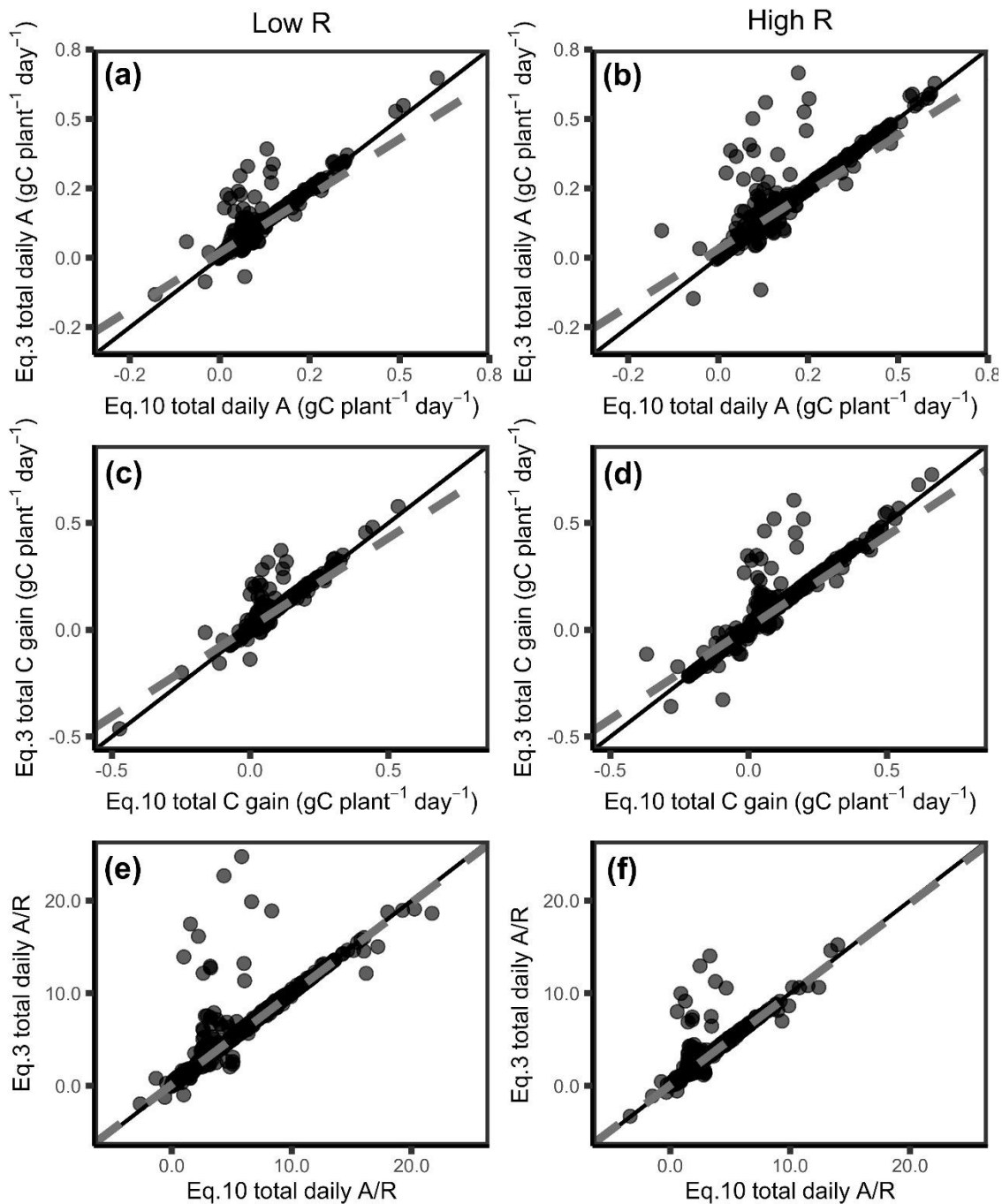


**Figure 4.** The modified Arrhenius equation without the missing term (Equation 3) gives differences in modelled daily carbon fluxes compared to Equation 10 for low R (a,c,e) and high R (b,d,f) under scenarios where  $H_d$  is allowed to vary. Modelled carbon fluxes include: a,b) Total daily photosynthesis; c,d) total daily C gain; and e,f) total daily A/R. A: photosynthesis, R respiration, Low R: low respiration, High R: high respiration. Black line indicates 1:1 line and grey dashed line indicates respective modelled slopes and intercepts.

372

373 **References**

- 374 **Amthor JS. 2000.** Direct effect of elevated CO<sub>2</sub> on nocturnal in situ leaf respiration in nine temperate  
375 deciduous tree species is small. *Tree Physiology* **20**: 139–144.
- 376 **Arrhenius S. 1915.** *Quantitative laws in biological chemistry*. Bell: London.
- 377 **Atkin OK, Tjoelker MG. 2003.** Thermal acclimation and the dynamic response of plant respiration to  
378 temperature. *Trends in Plant Science* **8**:343-351.
- 379 **Ayub G, Smith RA, Tissue DT, Atkin OK. 2011.** Impacts of drought on leaf respiration in darkness and  
380 light in *Eucalyptus saligna* exposed to industrial-age atmospheric CO<sub>2</sub> and growth temperature.  
381 *New Phytologist* **190**: 1003-1018.
- 382 **Bernacchi CJ, Singsaas EL, Pimentel C, Portis Jr AR, Long SP. 2001.** Improved temperature response  
383 functions for models of rubisco-limited photosynthesis. *Plant Cell and Environment* **24**:253-259.
- 384 **Blackman, VH. 1919.** The compound interest and plant growth. *Annals of Botany* **33**: 353-360.
- 385 **Causton, DR. 1991.** Plant-growth analysis: the variability of relative growth rate within a sample.  
386 *Annals of Botany* **67**(2): 137-144.
- 387 **Ciais P, Sabine C, Bala G, Bopp L, Brovkin V, Canadell J, Chhabra A, DeFries R, Galloway J, Heimann**  
388 **M. 2013.** Carbon and Other Biogeochemical Cycles. In: Heinze C, Tans P, Vesala T, eds. *Climate*  
389 *Change 2013: The Physical Science Basis*. Cambridge, UK, and New York, NY, USA: Cambridge  
390 University Press.
- 391 **Duursma RA, Medlyn BE. 2012.** MAESPA: a model to study interaction between water limitation,  
392 environmental drivers and vegetation function at tree and stand levels, with an example  
393 application to [CO<sub>2</sub>] x drought interactions. *Geoscientific Model Development* **5**:919-940.
- 394 **Elzhov TV, Mullen KM, Spiess A-N, Bolker B. 2016.** minpack.lm: R Interface to the Levenberg-  
395 Marquardt nonlinear least-squares algorithm found in MINPACK, plus support for bounds. R  
396 package version 1.2-1. <https://CRAN.R-project.org/package=minpack.lm>
- 397 **Farquhar GD, et al. 1980.** A biochemical model of photosynthetic CO<sub>2</sub> assimilation in leaves of C<sub>3</sub>  
398 species. *Planta* **149**: 78-90.
- 399 **Harley PC, Baldocchi DD. 1995.** Scaling carbon dioxide and water vapour exchange from leaf to  
400 canopy in a deciduous forest. I. Leaf model parameterization. *Plant, Cell and Environment*  
401 **18**:1146-1156.

402 **Harley PC, Thomas RB, Reynolds JF, Strain BR. 1992.** Modelling photosynthesis of cotton grown in  
 403 elevated CO<sub>2</sub>. *Plant, Cell and Environment* **15**:271-282.

404 **Harley PC, Tenhunen JD, Lange OL. 1986.** Use of an analytical model to study limitations on net  
 405 photosynthesis in *Arbutus unedo* under field conditions. *Oecologia* **70**:393-401.

406 **Heskel MA, O'Sullivan OS, Reich PB, Tjoelker MG, Weerasinghe LK, Penillard A, Egerton JG, et al.**  
 407 **2016.** Convergence in the temperature response of leaf respiration across biomes and plant  
 408 functional types. *Proceedings of the National Academy of Sciences USA* **113**: 3832-3837.

409 **Hobbs JK, Jiao W, Ester AD, Parker EJ, Schipper LA, Arcus VL. 2013.** Change in heat capacity for  
 410 enzyme catalysis determines temperature dependence of enzyme catalyzed rates. *ACS Chemical*  
 411 *Biology* **8**:2388-2392.

412 **Jensen JLWV. 1906.** Sur les fonctions convexes et les inégalités entre les valeurs moyennes. *Acta*  
 413 *Mathematica* **30**: 175-193.

414 **Johnson FH, Eyring H, Williams RW. 1942.** The nature of enzyme inhibitions in bacterial  
 415 luminescence: sulfanilamide, urethane, temperature and pressure. *Journal of Cellular and*  
 416 *Comparative Physiology* **20**:247-268.

417 **Kattge J, Knorr W. 2007.** Temperature acclimation in a biochemical model of photosynthesis: a  
 418 reanalysis of data from 36 species. *Plant, Cell and Environment* **30**:1176-1190.

419 **Kruse J, Hopmans P, Adams MA. 2008.** Temperature responses are a window to the physiology of  
 420 dark respiration: differences between CO<sub>2</sub> release and O<sub>2</sub> reduction shed light on energy  
 421 conservation. *Plant, Cell and Environment* **31**: 901-914.

422 **Kumarathunge DP, Medlyn BE, Drake JE, Tjoelker MG, Aspinwall MJ, Battaglia M, Cano FJ, Carter**  
 423 **KR, Molly AC, Lucas AC, et al. 2019.** Acclimation and adaptation components of the  
 424 temperature dependence of plant photosynthesis at the global scale. *New Phytologist* **222**:768-  
 425 784.

426 **Kumarathunge DP, Medlyn BE, Drake JE, Tjoelker MG, Aspinwall MJ, Battaglia M, Cano FJ, Carter**  
 427 **KR, Molly AC, Lucas AC, et al. 2018.** ACi-TGlob\_V1.0: a global dataset of photosynthetic CO<sub>2</sub>  
 428 response curves of terrestrial plants. doi: 10.6084/m9.figshare.7283567.v1.

429 **Lloyd J, Grace J, Miranda AC, Meir P, Wong SC, Miranda HS, Wright IR, Gash JHC, McIntyre J. 1995.** A  
 430 simple calibrated model of Amazon rainforest productivity based on leaf biochemical  
 431 properties. *Plant, Cell and Environment* **18**:1129-1145.

432 **Lombardozzi DL, Bonan GB, Smith NG, Dukes JS, Fisher RA. 2015.** Temperature acclimation of  
 433 photosynthesis and respiration: a key uncertainty in the carbon cycle-climate feedback.  
 434 *Geophysical Research Letters* **42**:8624-8631.

435 **Loveys BR, Atkinson LJ, Sherlock DJ, Roberts RL, Fitter AH, Atkin OK. 2003.** Thermal acclimation of  
 436 leaf and root respiration: An investigation comparing inherently fast- and slow-growing plant  
 437 species. *Global Change Biology* **9**(6): 895-910.

438 **Medlyn BE, Duursma RA, Eamus D, Ellsworth DS, Prentice IC, Barton CVM, Crous KY, et al. 2011.**  
 439 Reconciling the optimal and empirical approaches to modelling stomatal conductance. *Global*  
 440 *Change Biology* **17**:2134-2144.

441 **Medlyn BE, Dreyer E, Ellsworth D, Forstreuter M, Harley PC, Kirschbaum MUF, Le Roux X, et al.**  
 442 **2002.** Temperature responses of parameters of a biochemically based model of photosynthesis.  
 443 II. A review of experimental data. *Plant, Cell and Environment* **25**:1167-1179.

444 **Mercado LM, Medlyn BE, Huntingford C, Oliver RJ, Clark DB, Sitch S, Zelazowski P, Kattge J, Harper**  
 445 **AB, Cox PM. 2018.** Large sensitivity in land carbon storage due to geographical and temporal  
 446 variation in the thermal response of photosynthetic capacity. *New Phytologist* **218**:1462-1477.

447 **Norman JM, Campbell GS. 1998.** *An introduction to environmental biophysics*. New York NY: Springer.

448 **Oikawa PY, Jenerette GD, Knox SH, Sturtevant C, Verfaillie J, Dronova I, Poindexter CM, Eichelmann**  
 449 **E, Baldocchi DD. 2016.** Evaluation of a hierarchy of models reveals importance of substrate  
 450 limitation for predicting carbon dioxide and methane exchange in restored wetlands. *Journal of*  
 451 *Geophysical Research – Biogeosciences* **122**:145-167.

452 **Pommerening A, Muszta, A. 2015.** Methods of modelling relative growth rate. *Forest Ecosystems* **2**:5.

453 **Poorter H, Niklas KJ, Reich PB, Oleksyn J, Poot P, Mommer L. 2012.** Biomass allocation to leaves,  
 454 stem, and roots: meta-analyses of interspecific variation and environmental control. *New*  
 455 *Phytologist* **193**: 30-50.

456 **R Core Team. 2019.** R: A language and environment for statistical computing. R Foundation for  
 457 Statistical Computing, Vienna, Austria. URL <https://www.R-project.org/>.

458 **Rogers A, Medlyn BE, Dukes JS, Bonan G, von Caemmerer S, Dietze MC, Kattge J, et al. 2017.** A  
 459 roadmap for improving the representation of photosynthesis in Earth system models. *New*  
 460 *Phytologist* **213**:22-42.

461 **Shipley, B.** The use of above-ground maximum relative growth-rate as an accurate predictor of whole-  
 462 plant maximum relative growth-rate. *Functional Ecology* **3**(6): 771-775.

463 **Smith NG, Dukes JS. 2017.** Short-term acclimation to warmer temperatures accelerates leaf carbon  
 464 exchange processes across plant types. *Global Change Biology* **23**:4840-4853.

465 **Stinziano JR, Murphy BK. 2020.** arrhenius.comparison: comparing versions of the modified Arrhenius  
 466 equation. R package version 1.0.0.

467 **Stinziano JR, Way DA. 2017.** Autumn photosynthetic decline and growth cessation in seedlings of  
 468 white spruce are decoupled under warming and photoperiod manipulations. *Plant, Cell and*  
 469 *Environment* **40**:1296-1316.

470 **Stinziano JR, Way DA, Bauerle WL. 2018.** Improving models of photosynthetic thermal acclimation:  
 471 which parameters are most important and how many should be modified? *Global Change*  
 472 *Biology* **24**:1580-1598.

473 **Stinziano JR, Bauerle WL, Way DA. 2019.** Modelled net carbon gain responses to climate change in  
 474 boreal trees: impacts of photosynthetic parameter selection and acclimation. *Global Change*  
 475 *Biology* **25**:1445-1465.

476 **Tjoelker M, Oleksyn J, Reich P. 1999.** Acclimation of respiration to temperature and CO<sub>2</sub> in seedlings  
 477 of boreal tree species in relation to plant size and relative growth rate. *Global Change Biology*  
 478 **49**(6): 679-691.

479 **Way DA, Yamori W. 2014.** Thermal acclimation of photosynthesis: on the importance of adjusting our  
 480 definitions and accounting for thermal acclimation of respiration. *Photosynthesis Research*  
 481 **119**:89-100.

482 **Weger HG, Guy RD. 1991.** Cytochrome and alternative pathway respiration in white spruce (*Picea*  
 483 *glauca*) roots. Effects of growth and measurement temperature. *Physiologia Plantarum* **83**:675-  
 484 681.